buildings

MDPI

Article

A Circular Economy Approach to Cement Production: Integrating Untreated Moroccan EAF Steel Slag for Performance and Sustainability

Ikrame Hattab [1], Otmane Boudouch [2], Amine Naim [3] and Reda Elkacmi [1,*]

[1] Laboratory of Environmental, Ecological and Agro-Industrial Engineering, Faculty of Science and Technology, Sultan Moulay Slimane University, BP 592, Beni-Mellal 23000, Morocco; hattab.ikrame@usms.ac.ma
[2] Laboratory of Sciences and Technologies Team, Higher Education and Training School, Chouaib Doukkali University, BP 299, El Jadida 24000, Morocco; oboudouch@gmail.com
[3] Laboratory of Physico-Chemical Sciences, Faculty of Sciences FS Ben M'Sik, Hassan II University, BP 7955, Casablanca 20670, Morocco; aminaim@gmail.com
* Correspondence: redakcm@gmail.com

Abstract

Partial substitution of ordinary Portland cement (OPC) with supplementary cementitious materials is a key strategy for reducing the clinker factor and associated CO_2 emissions from cement production. This study investigates the feasibility of incorporating untreated electric arc furnace steel slag (EAF-SS), collected from a steel plant in Kenitra, Morocco, as a partial replacement of OPC in Portland cement. The material was characterized using X-ray diffraction (XRD), X-ray fluorescence (XRF), and particle size distribution (PSD) analysis. Cement blends containing 2–15 wt.% EAF-SS as a replacement of OPC were prepared and tested in accordance with EN standards to evaluate consistency, setting time, density, porosity, and compressive and flexural strengths at 2, 7, and 28 days. Increasing EAF-SS content from 2% to 15% slightly delayed the initial setting time by 3–17 min and reduced early-age compressive strength from 36 MPa for OPC to 26 MPa for the 15% blend at 2 days. At 28 days, mixtures containing 2–5% EAF-SS achieved compressive strengths of 42–52 MPa, satisfying class 42.5R requirements, whereas higher replacement levels (10–15%) reduced strength to 36–39 MPa. Flexural strength decreased from 7.5 MPa for OPC to 5.7 MPa for the 15% blend at 2 days and to 7.3 MPa at 28 days, while density decreased by 2–4% and total porosity increased from 12% to 18% with increasing slag content. Drying shrinkage decreased slightly with increasing EAF-SS content, from 630 μm/m for OPC to 560 μm/m for BC15 at 28 days, suggesting a modest beneficial effect on dimensional stability. The investigated slag exhibited an Fe_2O_3 content of ~57 wt.%, substantially higher than values commonly reported for many European and Chinese EAF slags. Accordingly, the novelty of the present work lies not simply in the geographical origin of the material, but in the standardized experimental assessment of a compositionally atypical, untreated, Fe-rich EAF steel slag used directly as a partial replacement of OPC in Portland cement. The study is intended as a first performance-oriented evaluation of this Moroccan by-product under EN-based testing conditions, rather than as a complete mechanistic or environmental assessment. These findings support the feasibility of low-level EAF-SS incorporation in blended cement and indicate a potential contribution to clinker factor reduction and associated CO_2 savings under the assumptions adopted in this study. However, the environmental benefit assessment remains preliminary and should be confirmed by full life-cycle and leaching analyses.

Check for updates

Academic Editor: Xiaoyong Wang

Received: 5 June 2026
Revised: 28 June 2026
Accepted: 3 July 2026
Published: 4 July 2026

Copyright: © 2026 by the authors. Licensee MDPI, Basel, Switzerland. This article is an open access article distributed under the terms and conditions of the Creative Commons Attribution (CC BY) license.

Keywords: cement hydration; circular economy; compressive strength; electric arc furnace steel slag (EAF-SS); flexural strength; setting time

1. Introduction

Cement is one of the most widely used basic materials in the world, with global cement consumption reaching approximately 4.00 billion tonnes in 2024, with projected growth of 5.24% between 2024 and 2030 [1]. In Morocco, cement deliveries reached about 12.3 million tonnes by the end of October 2025 [2].

Ordinary Portland cement (OPC) continues to dominate the civil engineering sector due to its versatility and mechanical performance [3]. However, the production of OPC relies heavily on clinkers, which is obtained by calcining limestone and clay at high temperatures [4] and is associated with significant environmental concerns. The cement industry accounts for nearly 7% of global industrial energy consumption and contributes around 8% of total anthropogenic CO_2 emissions, mainly due to clinker production and the decarbonation of limestone [5–8].

Given these environmental challenges, partially replacing OPC with supplementary cementitious materials (SCMs) has emerged as a promising pathway to reduce the carbon footprint of cement while preserving natural resources [9–12]. Various industrial and agricultural by-products, such as fly ash [13,14], rice husk ash [13], blast furnace slag [10,15,16], silica fume [17,18], and other waste-derived materials including ceramic powders and recycled crushed brick [11,12], have been successfully incorporated into cementitious mixtures, improving performance and reducing environmental impact. These composite systems enable a reduction in clinker consumption through lower OPC demand and support the integrated management of industrial waste, thereby aligning with circular economy principles [19–21].

Beyond single-component SCMs, recent studies have highlighted the synergistic valorization of multiple industrial solid waste streams—including red mud, iron ore tailings, and copper flotation tailings—in cementitious and geotechnical systems [22–24]. These works demonstrate that Fe-rich and compositionally atypical waste can be effectively integrated into construction materials, provided their specific mineralogical characteristics are thoroughly understood. However, the behavior of iron-oxide-rich slags such as Moroccan EAF-SS—with Fe_2O_3 contents far exceeding those of red mud or conventional EAF slags—remains largely unexplored as a standalone OPC replacement under standardized Portland cement conditions, motivating the present study.

Among traditional SCMs, steel slag represents a promising but underutilized material. Steelmaking generates large amounts of solid by-products, including slags, sludge, dust, and mill scale. Depending on the process, approximately 20 wt.% (electric arc furnaces, EAF) to 40 wt.% (basic oxygen furnaces, BOF) of steel by-products are generated per ton of steel [6]. According to the World Steel Association, global crude steel production reached 161.6 million tons in May 2023 [19]. EAF slag has a chemical composition rich in calcium silicates and ferrites, similar to some of the mineral phases present in OPC clinker, suggesting its potential suitability as a partial OPC replacement in blended cement systems [6,25]. However, its reactivity is generally lower than that of other SCMs, and several studies have reported delayed hydration, reduced early compressive strength, and changes in setting behavior when using untreated EAF-SS [20,21,26,27]. Surface treatments such as carbonation have been proposed to improve its reactivity and reduce volume instability [28–30].

In Morocco, the steel industry has experienced significant growth over the past two decades, mainly due to the adoption of EAF processes [6,20,21,25]. This growth has resulted in the annual production of nearly 196,000 tonnes of EAF steel slag, most of which is stored in landfills near production sites [6,20,21]. Although the management of this waste poses environmental and logistical challenges, it also presents a valuable opportunity for recycling EAF slag in cement production.

While the utilization of EAF steel slag as a supplementary cementitious material has been investigated in several international studies, the large majority of published work focuses either on blast furnace slag, chemically or mechanically activated EAF slags, or slags produced under European and Asian industrial conditions. In contrast, Moroccan EAF-SS exhibits a distinctly different chemical profile, characterized by an exceptionally high Fe_2O_3 content (~57 wt%) and relatively low SiO_2 (~6 wt%), which differs substantially from European slags (~15–20 wt% Fe_2O_3) and Chinese slags (~16–20 wt% Fe_2O_3) reported in the literature. This Fe- and Mg-rich mineralogical signature, dominated by wüstite (FeO), periclase (MgO), and calcium silicate phases, differs substantially from previously studied EAF slags in terms of chemical composition and phase assemblage, thereby motivating a dedicated standardized performance assessment under EN 197-1 conditions. Furthermore, the direct use of untreated Moroccan EAF-SS, without any chemical or mechanical activation, represents a practically relevant and underexplored approach, particularly given the annual accumulation of nearly 196,000 tonnes of this material in Moroccan landfills. Accordingly, the novelty of the present work lies not in proposing new hydration mechanisms or high substitution rates, but in providing a standardized performance-oriented assessment of an untreated and compositionally atypical Moroccan EAF steel slag used directly as a low-level OPC replacement, together with a critical discussion of how its mineralogical characteristics may relate to the observed early-age behavior. By providing standardized experimental data on this compositionally distinct and regionally specific slag, this study offers new insights that complement the existing literature on EAF slag valorization in cementitious systems.

Therefore, the main objective of this study is to evaluate the engineering feasibility of incorporating untreated Moroccan EAF steel slag as a low-level partial replacement of ordinary Portland cement in blended cement systems. The study focuses on the influence of EAF-SS incorporation on key cement properties, including water demand, setting time, mechanical strength, density, porosity, and drying shrinkage, while relating the observed macroscopic behavior to the mineralogical characteristics of the slag. By providing experimental data on the performance of untreated Moroccan EAF steel slag under standardized testing conditions, this work contributes to the sustainable valorization of steelmaking by-products and supports the development of low-carbon cementitious materials within a circular economy framework.

In addition, pore-solution pH evolution is reported as a supplementary empirical observation, without direct mechanistic verification.

2. Materials and Methods

2.1. Materials

Electric arc furnace steel slags (EAF-SS) were collected from a Moroccan Steel plant operating an electric arc furnace, then homogenized, crushed and sieved to obtain a particle size distribution suitable for cement production.

The chemical composition of EAF-SS was analyzed by X-ray fluorescence (XRF) using an Epsilon4 **X-ray fluorescence spectrometer (Malvern Panalytical, Almelo, The Netherlands)** (Table 1). EAF-SS is mainly composed of Fe_2O_3 and CaO with relatively low SiO_2 content. While these major oxide families are broadly consistent with the general chemistry of EAF

slags reported in the literature [6,21], the exceptionally high Fe_2O_3 content highlights the compositionally atypical nature of the Moroccan slag investigated in this study.

Table 1. Chemical composition of EAF-SS.

Oxide Content (wt%)	Fe_2O_3	CaO	SiO_2	MgO	Al_2O_3	MnO	Cr_2O_3	P_2O_5	SO_3	TiO_2	CuO	NiO	Na_2O
EAF-SS	57.12	27.18	5.87	2.39	1.43	3.16	0.89	0.30	0.16	0.35	0.08	0.08	0.03

In addition to the major oxides, the EAF-SS contains minor and trace elements such as Cr_2O_3, CuO, NiO, MnO, and P_2O_5. These components are typical of EAF steel slags and originate from alloying elements and raw materials used in steel production. Their concentrations remain low and are consistent with values reported in the literature [6,21].

2.2. Experimental Methods

The chemical composition of EAF-SS was determined by X-ray fluorescence (XRF) using an Epsilon4 spectrometer (Malvern Panalytical, Almelo, The Netherlands).

Mineralogical phases were identified by X-ray diffraction (XRD) using a PANalytical X'Pert PRO (Malvern Panalytical, Almelo, The Netherlands) diffractometer equipped with Cu-Kα radiation (λ = 1.5406 Å, 40 kV, 40 mA). Scans were performed from 10° to 80° (2θ) with a step size of 0.02° and a scan speed of 2°/min. Phase identification was carried out using HighScore Plus software (Version 4.9, Malvern Panalytical, Almelo, The Netherlands) and the ICDD database, allowing identification of major crystalline phases such as dicalcium silicate (C_2S), tricalcium silicate (C_3S), calcium ferrite (C_4AF), and lime (CaO).

Particle size distribution (PSD) was determined using a Master sizer 3000 laser diffraction analyzer (Malvern Panalytical, Malvern, UK) in dry mode after ultrasonic dispersion to prevent particle agglomeration. Characteristic diameters (d_{10}, d_{50}, d_{90}) were calculated from cumulative volume distributions.

The specific surface area (SSA) was measured using the Brunauer–Emmett–Teller (BET) method with nitrogen adsorption on an ASAP 2020 analyzer (Micromeritics Instrument Corporation, Norcross, GA, USA) after degassing samples at 120 °C for 12 h.

2.3. Mixture Proportions

Six cement blends were prepared to investigate the effect of EAF-SS on physico-mechanical properties. A control mix (OPC) consisted of 100 wt% ordinary Portland cement. The other five mixtures partially replaced OPC with EAF-SS at 2, 3, 5, 10, and 15 wt%. These substitution levels were selected based on both industrial feasibility and previous studies on partial replacement of OPC with electric arc furnace steel slag, which demonstrated acceptable mechanical performance and workability within this range [6,21]. Mix proportions are given in Table 2.

Table 2. Cement blend compositions (wt%).

Sample Code	% by Weight of OPC	% by Weight of EAF-SS
OPC	100	0
BC2	98	2
BC3	97	3
BC5	95	5
BC10	90	10
BC15	85	15

2.3.1. Mortar Preparation

Mortars were prepared using blended cements, natural siliceous sand (≥97% SiO_2), and potable water. The sand water content was <0.2%, determined by drying at 105–110 °C for 2 h. Mortars were mixed at a ratio of 1 part cement:3 parts sand:0.5 parts water by mass. All materials were at laboratory temperature for homogeneous mixing.

2.3.2. Specimen Preparation and Curing

Standard mortar prisms (40 × 40 × 160 mm^3) were cast for compressive and flexural strength tests. Specimens were cured in a humid atmosphere for 24 h, demolded, and stored in water until testing at 2, 7, and 28 days. Three specimens were prepared for each mixture and testing age. Sand particle size distribution is summarized in Table 3.

Table 3. Sand particle size distribution.

Sieve Size (mm)	Cumulative Retained (%)
2.00	0
1.60	7 ± 5
1.00	33 ± 5
0.50	67 ± 5
0.16	87 ± 5
0.08	99 ± 5

2.3.3. Open Porosity Measurement

The open porosity of mortar specimens was measured using a gravimetric water immersion method in accordance with NF P 18-459 [31]. Samples were first oven-dried at 105 °C for 24 h and weighed to obtain the dry mass (Md). The specimens were then immersed in water under vacuum to ensure complete saturation of accessible pores. The saturated mass in air (Ms) and the apparent mass in water (Mw) were subsequently recorded. The open porosity was calculated as:

$$\text{Porosity (\%)} = (\text{Ms} - \text{Md})/(\text{Ms} - \text{Mw}) \times 100$$

This method provides a reproducible estimate of the fraction of pore volume accessible to water. It should be noted that this technique measures only open porosity and does not account for closed pores, total pore volume, or pore size distribution.

2.4. Pore Solution pH Measurement

The evolution of pore solution pH was measured to investigate the effect of EAF-SS on early hydration and setting time. Cement pastes were prepared using OPC and EAF-SS blended cements at replacement levels of 2%, 3%, 5%, 10%, and 15% by weight. Each paste was mixed with water at the water-to-cement ratio determined to achieve normal consistency.

Samples of pore solution were extracted at selected hydration times (0.5 h, 1–2 h, 4–8 h, and 24 h) using a vacuum filtration technique to separate the liquid phase. The filtration process was completed within 2–3 min to minimize the risk of continued hydration during extraction. While some degree of continued reaction cannot be entirely excluded, this source of uncertainty is common to all pore solution extraction methods and is considered negligible relative to the pH differences observed between OPC and EAF-SS blended systems. The pH of the pore solution was measured immediately after extraction using a calibrated pH meter at room temperature (25 ± 1 °C). Measurements were performed in

triplicate for each sample to ensure reproducibility, and the average valueswere used for data analysis.

2.5. Durability-Shrinkage Test

Shrinkage of OPC and EAF-SS blended mortars was measured according to the Moroccan standard NM 10.1.005 [32]. Mortar prisms ($40 \times 40 \times 160$ mm^3) were prepared using the same mix proportions as described in Section 2.3. After casting, specimens were cured in a humid chamber for 24 h, demolded, and then stored under controlled conditions (20 ± 2 °C, 50 ± 5% relative humidity (RH)) until testing.

Shrinkage measurements were performed on three prism specimens for each mixture, and the reported values correspond to the average shrinkage with the associated standard deviation.

Linear shrinkage was monitored at selected ages (1, 3, 7, 14, and 28 days) using a length comparator, following the procedure specified in NM 10.1.00529. Three specimens were tested for each mixture, and the average values were reported.

3. Results & Discussion

3.1. XRD Analysis of EAF-SS

Figure 1 presents the X-ray diffraction (XRD) pattern of Moroccan electric arc furnace steel slag (EAF-SS). Major crystalline phases identified include β-C_2S (belite) and C_3S (alite) at $2\theta \approx 32$–$34°$, FeO (wüstite) at 42.9° and 62.4°, and MgO (periclase) at 78.6° (Table 4). The peak previously assigned to C_4AF (~50°) does not match its characteristic reflections (ICDD PDF 01-071-0667) and may correspond to minor Fe-rich phases. All peaks were confirmed using ICDD reference patterns.

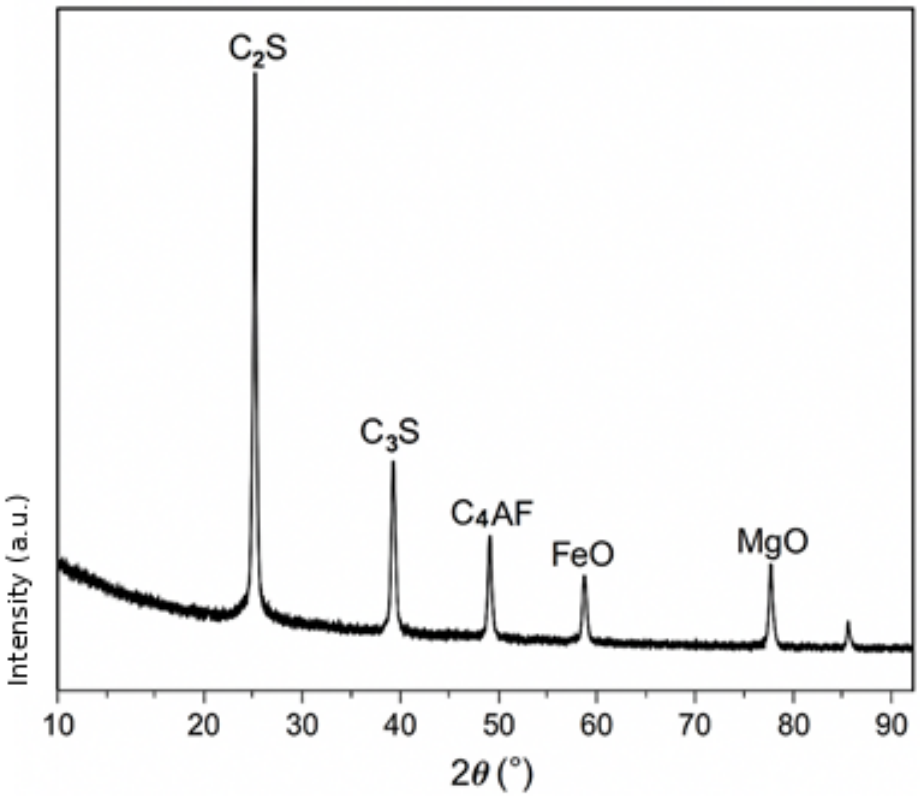


Figure 1. XRD pattern of Moroccan EAF-SS.

Table 4. XRD peak assignments for Moroccan EAF-SS.

Mineral Phase	2θ (°) (Experimental)	d-Spacing (Å) (Calculated)	ICDD PDF Reference	Comments
β-C_2S (Belite) + C_3S (Alite)	32.2	2.78	01-083-0460 (C_2S) + 01-073-0599 (C_3S)	Overlapping reflections from both calcium silicates
C_3S (Alite)	34.5	2.60	01-073-0599	Additional characteristic peak of alite
FeO (Wüstite)	42.9	2.11	01-089-0687	Main reflection of wüstite
FeO (Wüstite)	62.4	1.49	01-089-0687	Secondary reflection of wüstite
MgO (Periclase)	78.6	1.22	01-075-1525	Characteristic peak of periclase

Semi-quantitative analysis of the crystalline fraction was performed using a relative intensity approach. The integrated peak areas of the main reflections corresponding to β-C_2S, C_3S, and Fe/Mg oxides were measured and normalized with respect to the total area of all identified crystalline peaks. The proportion of each phase was estimated using the following expression:

$$\text{Phase fraction (\%)} = (\text{Peak area of phase}/\text{Sum of all crystalline peak areas}) \times 100$$

This method provides an approximate estimation of the relative abundance of crystalline phases, assuming that peak intensities are proportional to phase content. Using this approach, β-C_2S was estimated at ~35% of the crystalline fraction, while C_3S and Fe/Mg oxides each represent ~20%, with the remainder attributed to minor or amorphous phases.

It should be emphasized that these values are approximate indicators rather than precise quantifications, as this semi-quantitative approach does not account for amorphous content and assumes similar crystallinity and scattering factors among phases, as commonly reported in previous studies [33–35]. Full Rietveld refinement is recommended in future studies to obtain more accurate quantitative phase compositions and confirm polymorph distributions.

The amorphous phase content was not quantified in this study, which represents a limitation in the assessment of EAF-SS reactivity. Therefore, the XRD results were used only to identify the main crystalline phases present in the slag, while the interpretation of hydration behavior and mechanical performance was based primarily on the experimental results obtained for the blended cements. Future work using internal standard methods or Rietveld refinement with amorphous phase quantification is recommended to provide a more complete characterization of the slag's reactive potential.

The identification of calcium silicate phases (C_2S and C_3S) indicates that the slag contains mineral phases commonly associated with hydraulic behavior. However, the actual reactivity of these phases was not quantified in the present study, and the polymorphic form of C_2S was not experimentally determined. Therefore, no specific conclusion is drawn regarding the hydraulic reactivity of these silicate phases, and their contribution to cement hydration should be regarded as a plausible but unverified interpretation. Further analyses such as high-resolution XRD or Raman spectroscopy would be required to confirm C_2S polymorph distribution and better assess slag reactivity.

The coexistence of calcium silicate phases (C_2S and C_3S) with Fe- and Mg-bearing compounds indicates a mineralogical assemblage that may influence the hydration behavior of slag-containing binders. In the present study, the lower early-age performance observed

for the EAF-SS blends may be qualitatively associated with this phase assemblage, together with the coarser particle size and lower specific surface area of the slag [6,36]. However, the specific role of Fe- and Mg-bearing phases was not directly investigated, and no mechanistic conclusions can be drawn in the absence of complementary analyses such as SEM, TGA, or calorimetry. In addition, the relatively low content of reactive amorphous phases suggests that optimal performance may require specific processing or activation treatments [3].

These observations are consistent with previous studies describing the general behavior of EAF slags in cement systems. Nguyen et al. [33] reported the persistence of C_2S- and ferrite-related phases in steel slags used as supplementary cementitious materials, while Andersson et al. [34] and Liu et al. [35] described mineralogical assemblages containing belite, ferrite, and Fe-rich phases in EAF slag systems. Together, these studies provide a relevant literature context for the mineralogical profile of Moroccan EAF-SS. However, direct comparison with hydrated paste XRD at 7 or 28 days was not performed in the present work, and such analysis is recommended in future studies to monitor phase evolution and hydration product formation more directly.

Overall, the XRD results provide a mineralogical framework for interpreting the behavior of Moroccan EAF-SS in blended cement systems. In combination with the physical and mechanical results discussed in later sections, these observations support the conclusion that low replacement levels (2–5 wt.%) provide the most favorable balance between clinker reduction and mechanical performance under the conditions investigated, while remaining compatible with the requirements of EN 197-1 class 42.5R [37] (Section 3.5).

3.2. Particle Size Distribution and Specific Surface Area Analyses

The physical characteristics of EAF-SS, particularly its particle size distribution and specific surface area, play crucial roles in determining its hydraulic behavior. Figure 2 presents the cumulative particle size distributions for both OPC and EAF-SS, showing significant differences in granulometry. The OPC exhibits a finer and more uniform particle distribution, with its curve positioned notably to the left of the EAF-SS distribution.

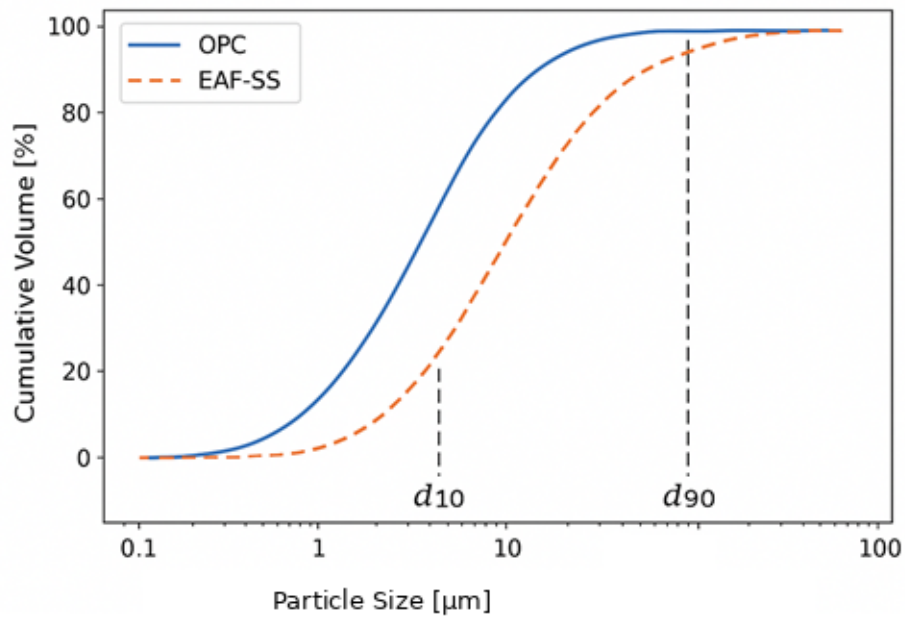


Figure 2. Cumulative particle size distribution curves of OPC and EAF-SS.

Quantitative analysis indicates median particle diameters (d_{50}) of approximately 16 µm for OPC and 32 µm for EAF-SS, confirming the significantly coarser nature of the steel slag. Similarly, the d90 value of EAF-SS is nearly twice that of OPC, highlighting the

presence of a higher fraction of coarse particles. This difference in granulometry directly affects the available reactive surface area and consequently the hydration kinetics of the blended system.

The broader particle size distribution of the EAF-SS reflects its lower grinding efficiency and the intrinsic heterogeneity of steel slag particles, which contain Fe-rich and Mg-rich crystalline phases that are more resistant to fragmentation.

This coarser texture reduces the total reactive surface available for dissolution of silicate phases during the initial hydration stage. As a result, the rate of ion release (Ca^{2+} and SiO_4^{4-}) into the pore solution is reduced, leading to slower nucleation of Calcium Silicate Hydrate C–S–H during the early hydration period, which contributes to the delayed setting time discussed in Section 3.4.

Table 5 summarizes the BET specific surface area measurements, which further highlight the distinct physical properties of the two materials. The EAF-SS displays a specific surface area of 0.92 m^2/g, substantially lower than the 1.85 m^2/g measured for OPC. The approximately two-fold reduction in surface area significantly limits the number of potential nucleation sites available for early C–S–H precipitation. This difference can be attributed to the denser crystalline structure and different fracture mechanics of the slag particles during grinding [20,31].

Table 5. Specific surface area of OPC and EAF-SS.

Material	Specific Surface Area (m^2/g)
OPC	1.85
EAF-SS	0.92

The lower SSA limits the number of nucleation sites for C–S–H (calcium silicate hydrate) formation during the initial hydration period.

Consequently, during the early hydration period, EAF-SS behaves primarily as a weakly reactive hydraulic filler, improving particle packing within the cement matrix and reducing initial porosity rather than directly contributing to early strength development.

However, the presence of intermediate-size particles (10–30 μm) combined with the hydraulic phases identified by XRD (β-C_2S and ferrite phases) may allow EAF-SS to contribute to later-age hydration, which could partly explain the gradual improvement in mechanical performance observed at 28 days. However, this interpretation remains qualitative because no calorimetric or microstructural analyses were performed.

Table 6 further confirms that EAF-SS particles are significantly coarser, as reflected by the higher D10, D50, D90, and mean particle-size values. This coarser particle-size distribution, together with the lower SSA reported in Table 5, explains the slower dissolution rate of reactive phases and the reduced early hydration reactivity of slag-containing systems.

Table 6. Particle size distribution of the clinker and EAF-SS.

Parameter	OPC Clinker	EAF-SS
D10 (μm)	4–6	10–14
D50 (μm)	14–18	28–35
D90 (μm)	28–32	55–70
Mean particle size (μm)	18–20	35–45

These findings are consistent with established principles of cement hydration, where particle fineness and surface area strongly control dissolution kinetics, nucleation of hydration products, and microstructural evolution in blended cement systems [36,38].

Therefore, both particle size distribution and specific surface area analyses confirm that the physical characteristics of EAF-SS contribute to slower early hydration but support microstructural densification at later curing ages.

3.3. Chemical Composition of Cement Samples

The X-ray fluorescence (XRF) analysis of OPC and blended cement samples (Table 7) shows that partial replacement of OPC with Moroccan EAF steel slag (EAF-SS) results in a progressive increase in Al_2O_3, Fe_2O_3, and MgO contents, accompanied by a moderate decrease in CaO. For instance, Fe_2O_3 increases from 3.45 wt% in OPC to 8.85 wt% in BC15, while MgO rises from 1.75 wt% to 2.42 wt%, reflecting the intrinsic mineralogy of EAF-SS. These compositional variations are consistent with the XRD results, which identified ferrite-rich phases (C_4AF) and Mg-bearing minerals such as periclase.

Table 7. Chemical composition of OPC and blended cement samples.

Oxide Content (wt%)	SiO_2	Al_2O_3	Fe_2O_3	CaO	MgO	K_2O	Na_2O	P_2O_5	MnO	SO_3	TiO_2	LOI *
OPC	19.94	4.65	3.45	63.10	1.75	1.37	0.21	0.11	0.03	3.01	0.21	1.96
BC2	19.80	4.72	3.90	62.85	1.79	1.35	0.21	0.11	0.09	2.99	0.24	1.77
BC3	19.90	4.80	4.44	61.70	1.90	1.35	0.21	0.12	0.15	2.97	0.37	1.88
BC5	19.82	4.89	4.79	61.05	1.95	1.32	0.23	0.17	0.27	3.06	0.51	1.77
BC10	19.84	5.11	6.61	59.59	2.15	1.31	0.21	0.14	0.48	2.64	0.31	1.41
BC15	19.78	5.52	8.85	56.69	2.42	1.33	0.21	0.15	0.75	2.47	0.32	1.31

* LOI: loss on ignition.

The alkali oxides Na_2O and K_2O remain nearly constant across all mixtures, indicating that EAF-SS incorporation did not significantly increase the alkali content of the blended cements. However, no dedicated alkali–silica reaction (ASR) tests were performed in the present study; therefore, no direct conclusion can be drawn regarding ASR risk in concrete applications, even though similar steel-slag-based binders have been discussed in the literature in this context [39].

Both the loss on ignition (LOI) and SO_3 contents remain below the maximum limits established by EN 197-1 (5% for LOI and 4% for SO_3). In the present study, LOI values vary between 1.31 and 1.96 wt%, while SO_3 contents remain between 2.47 and 3.06 wt%, confirming the chemical stability of the blended systems and the absence of excessive free lime, residual carbon, or moisture-related instabilities [40].

The gradual increase in Fe_2O_3 content is particularly relevant for understanding the hydration behavior of the blended cements. Iron-rich phases may contribute to the formation of Fe-enriched surface layers during the early stages of hydration, which can reduce the dissolution rate of reactive silicates and delay the nucleation of C–S–H [40–42]. This mechanism can partially explain the longer setting time and reduced early-age strength observed in the mechanical tests (Section 3.5). Similar effects have been reported in previous studies investigating the hydration behavior of Fe-rich steel slags [6,21,43].

At the same time, the moderate MgO content remains within acceptable limits for cementitious materials. Although MgO can potentially hydrate to form brucite, the relatively low concentration observed here ($\leq$2.42 wt%) minimizes the risk of deleterious expansion while still contributing to slower early hydration kinetics.

The SiO_2 content remains relatively constant (~19.8 wt%), which indicates that EAF-SS does not significantly increase the amorphous silica fraction of the binder. Consequently, its pozzolanic reactivity is expected to be lower than that of blast furnace slag, which typically contains more than 30 wt% amorphous SiO_2 [40]. Instead, the slag behaves mainly as a slow-reacting hydraulic component, where belite-type phases and ferrites contribute gradually to hydration reactions.

Overall, the chemical composition confirms that Moroccan EAF-SS behaves primarily as a slow-reacting hydraulic material with limited pozzolanic activity, but capable of contributing to long-term microstructural densification. These characteristics support its use as a partial replacement of OPC up to 15%, while maintaining compliance with the chemical requirements of EN 197-1 [37].

The progressive increase in Fe_2O_3 and MgO with increasing slag content confirms the successful incorporation of EAF-SS into the blended cement matrix.

3.4. Normal Consistency and Initial Setting Time

Table 8 summarizes the water-to-cement ratio (W/C) required to achieve normal consistency, together with the corresponding initial setting times of the investigated binders. The results (Table 8, Figure 3) indicate that increasing the proportion of EAF-SS progressively reduced the water demand, with W/C decreasing from 27.53% for OPC to 24.81% for BC15. This reduction may be attributed primarily to the physical characteristics of the slag particles, particularly their lower specific surface area and lower water demand compared with clinker. As shown by the particle size distribution and BET analyses (Section 3.2), EAF-SS particles are relatively coarser and exhibit a lower specific surface area than OPC, which likely reduces their capacity to retain mixing water. In addition, partial replacement of clinker by coarser slag particles may modify particle packing within the binder system, thereby contributing to the lower water requirement observed. Similar reductions in water demand have been reported for EAF slag used in blended cement systems [44,45].

Table 8. Water-to-cement ratio (W/C)% and initial setting time of samples.

Sample Code	Water-to-Cement Ratio (W/C)%	Initial Setting Time (min)
OPC	27.53	145
BC2	26.79	148
BC3	26.56	150
BC5	26.15	155
BC10	25.41	157
BC15	24.81	162

In contrast, the initial setting time increases gradually with increasing slag content, rising from 145 min for OPC to 162 min for BC15. Although this increase remains within acceptable limits for cementitious binders, it reflects a moderate retardation of early hydration reactions in the slag-blended systems.

Several factors may contribute to this behavior. First, partial replacement of OPC by untreated EAF-SS reduces the proportion of readily reactive clinker phases available during the early hydration period. In addition, the slag itself appears to contribute less to early-age hydration than OPC under the present test conditions, as suggested by its mineralogical characteristics and the lower early-age performance observed in the blended systems. Together, these effects may slow the rate of early hydration and delay the formation of hydration products governing initial stiffening and setting.

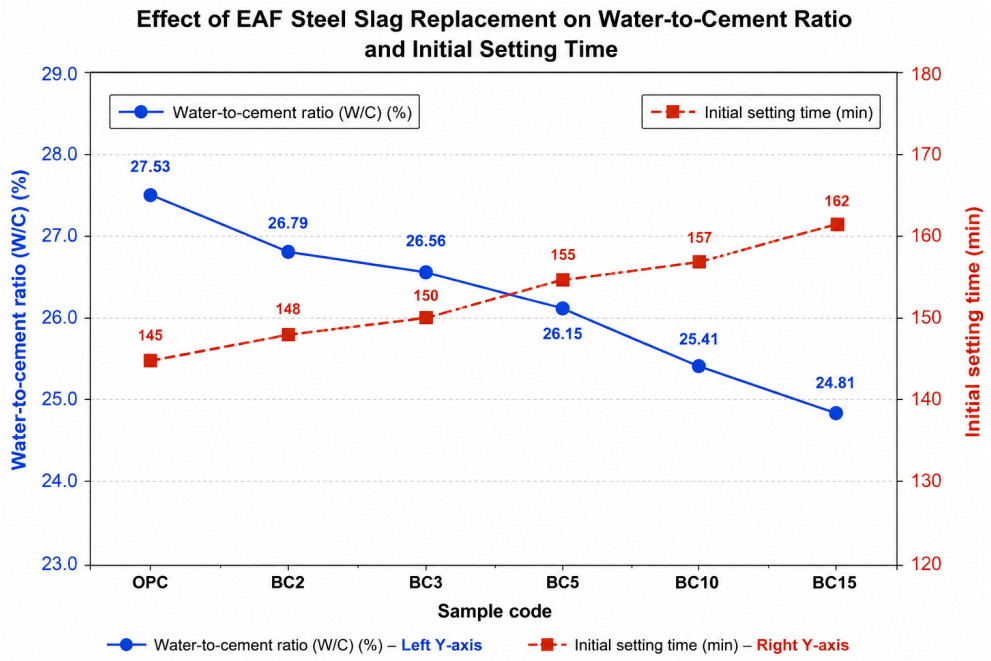


Figure 3. Water-to-cement ratio and initial setting time of samples.

To further examine the early hydration environment, the pH of the pore solution was measured at different times (0.5 h, 1–2 h, 4–8 h, and 24 h) for OPC and EAF-SS blended cements. The results (Table 9) show that slag-containing binders, particularly at higher replacement levels (10–15%), exhibited lower initial pH values and a slower increase in pH during the first 24 h compared with OPC. Low-dosage blends (2–5%) showed a smaller pH decrease and correspondingly smaller delays in initial setting time.

Table 9. Evolution of pore solution pH for OPC and EAF-SS blended cements at different hydration times.

Samples	0.5 h	1–2 h	4–8 h	24 h
OPC	11.4	12.3	13.0	13.0
EAF-SS blended cement (2–5%)	11.0	11.5	12.0	12.5
EAF-SS blended cement (10–15%)	10.5	11.0	11.5	12.0

These results suggest that the incorporation of EAF-SS modifies the early pore-solution chemistry of the blended binder, which may contribute to the observed delay in setting. However, the present data do not allow the specific contribution of Fe-rich phases, Mg-bearing phases, free lime, or sulfate–aluminate interactions to be isolated. Likewise, ionic concentrations (e.g., Ca^{2+}, Fe^{2+}/Fe^{3+}) were not measured, and no formal statistical correlation analysis between pH evolution and setting time was performed. Therefore, the relationship between reduced pH and delayed setting should be regarded as a qualitative interpretation based on parallel experimental trends rather than as a directly verified mechanistic proof.

It is also possible that the observed retardation reflects the combined influence of clinker dilution, the limited early contribution of slag hydration, and modified pore-solution chemistry rather than a single controlling mechanism. In addition, because no inert filler reference material (e.g., limestone powder) was included in the experimental program, the respective contributions of physical dilution/filler effects and slag-specific chemical effects could not be fully separated in the present study.

Overall, the results show that untreated Moroccan EAF-SS reduces water demand while slightly extending the initial setting time of blended cements. Under the conditions investigated, this setting delay remained moderate and within acceptable practical limits. The observed trends are consistent with previous reports on EAF slag-containing binders [40,43,44], although direct confirmation of the underlying hydration mechanisms will require complementary analyses such as ionic monitoring, calorimetry, and microstructural characterization.

3.5. Compressive-Flexure Strength and Open Porosity

The compressive and flexural strength results of OPC and EAF-SS–blended cements are summarized in Table 10. Increasing EAF-SS content progressively reduces early-age compressive strength. At 2 days, compressive strength decreases from 36 MPa for OPC to 26 MPa for BC15, corresponding to a strength retention of 72%. At 7 days, it decreases from 46 MPa to 32 MPa (retention 70%), and at 28 days, from 53 MPa to 36 MPa (retention 68%). Flexural strength follows a similar trend, indicating that early mechanical performance is strongly influenced by the amount of clinker replacement.

Table 10. Compressive and flexural strength and porosity.

Sample Code	EAF-SS (%)	Compressive Strength (MPa)			Flexural Strength (MPa)			Density (g/cm^3)	Porosity (%)
		2 Days	7 Days	28 Days	2 Days	7 Days	28 Days		
OPC	0	36.0 ± 0.2	46.0 ± 0.2	53.0 ± 0.5	7.5 ± 0.03	9.2 ± 0.02	9.0 ± 0.02	2.78 ± 0.03	12.0 ± 0.7
BC2	2	35 ± 0.2	45.0 ± 0.2	52.0 ± 0.5	7.3 ± 0.03	9.0 ± 0.02	9.0 ± 0.02	2.78 ± 0.03	13.0 ± 0.7
BC3	3	31.0 ± 0.2	38.0 ± 0.5	44.0 ± 0.4	6.6 ± 0.02	7.8 ± 0.03	8.9 ± 0.03	2.74 ± 0.02	14.0 ± 0.5
BC5	5	29.0 ± 0.5	36.0 ± 0.5	42.5 ± 0.4	6.2 ± 0.02	7.4 ± 0.02	8.5 ± 0.03	2.72 ± 0.02	15.0 ± 0.6
BC10	10	28.0 ± 0.3	34.0 ± 0.3	39.0 ± 0.2	6.0 ± 0.02	7.0 ± 0.03	8.0 ± 0.02	2.68 ± 0.02	17.0 ± 0.4
BC15	15	26.0 ± 0.2	32.0 ± 0.2	36.0 ± 0.2	5.7 ± 0.02	6.7 ± 0.03	7.3 ± 0.02	2.65 ± 0.02	18.0 ± 0.4

At 28 days, the strength reduction becomes less pronounced, indicating a partial recovery of mechanical performance over time. This trend may be consistent with a progressive contribution of the slag-containing system to later-age hardening; however, no direct hydration-kinetics or microstructural measurements were performed to verify the underlying mechanism. Direct hydration kinetics measurements (e.g., isothermal calorimetry or TGA) were not conducted; therefore, terms such as "delayed hydration" and "Fe-rich phase passivation" are presented cautiously, reflecting plausible mechanisms rather than experimentally verified kinetics.

The reduction in mechanical strength is likely related to both the mineralogical composition and the physical characteristics of untreated EAF-SS. XRD analysis identified calcium silicate phases together with Fe- and Mg-bearing crystalline phases in the slag. However, because the phase assemblage was estimated using a semi-quantitative approach and the amorphous phase content was not determined, these results should be interpreted primarily as mineralogical indicators rather than as rigorous quantitative evidence of reactivity. In particular, although calcium silicate phases such as C_2S and C_3S were identified, their exact contribution to hydration and strength development could not be established directly in the absence of calorimetric or thermogravimetric measurements. The presence of Fe- and Mg-bearing phases may also influence the hydration behavior of the blended system, but their specific role in early-age strength development was not directly verified in this study. Therefore, the observed strength loss should be interpreted as the result of the combined effects of clinker dilution, lower early-age slag reactivity, and the physical characteristics of the slag particles, rather than being attributed to a single identified mechanism.

In addition to mineralogical aspects, the physical characteristics of EAF-SS are also likely to influence mechanical behavior. The particle size distribution and BET results indicate that the slag is coarser and has a lower specific surface area than OPC, which reduces the available reactive surface and may limit early hydration and packing efficiency in the blended systems. These physical characteristics may contribute to the observed increase in porosity and reduction in mechanical strength at higher replacement levels, in agreement with trends reported for steel slag blended binders in previous studies [46].

However, no direct microstructural observations of the interfacial transition zone were performed; therefore, any discussion of ITZ defects or particle–matrix bonding remains hypothetical.

Density and open porosity measurements (Table 10) further illustrate the effect of slag content. As slag content increases from 0% to 15%, density decreases from 2.78 to 2.65 g/cm^3, while open porosity rises from 12% to 18%. The relationship between strength reduction and porosity is illustrated by the 28-day compressive strength retention, decreasing from 100% (OPC) to 68% (BC15). Linear regression of compressive strength versus total porosity shows a strong negative correlation, described by:

$$fc = -2.85P + 86.75 \ (R^2 = 0.95)$$

where fc is the 28-day compressive strength (MPa) and P is the open porosity (%). This strong negative correlation indicates that higher open porosity is closely associated with lower 28-day compressive strength in the investigated mixtures. Although correlation does not by itself establish causality, the result supports the interpretation that pore structure is a key factor governing strength loss in the slag-blended systems.

Taken together, the strength, porosity, and compositional results suggest that the observed reduction in mechanical performance arises from a combination of clinker dilution, the limited early hydraulic contribution of untreated EAF-SS under the present conditions, and the physical characteristics of the slag particles. However, the present experimental program does not allow these two contributions to be quantitatively separated. Likewise, although lower replacement levels may benefit from improved particle packing, no inert filler reference was included; therefore, a true filler effect could not be demonstrated directly in this study, even if similar packing-related contributions have been discussed in the literature [47].

Overall, the combined analysis of mechanical strength, density, porosity, and strength retention indicates that Moroccan EAF-SS can be incorporated into Portland cement at low substitution levels. Under the investigated conditions, the most technically suitable range is 2–5 wt.% EAF-SS, which satisfies the mechanical requirements of strength class 42.5R at 28 days. Higher replacement levels (10–15 wt.%) remain useful for understanding the performance limits of the system, but they led to significant strength reductions and cannot be recommended for 42.5R-equivalent applications based on the present results.

3.6. Volume Stability and Early-Age Shrinkage Behavior

Drying shrinkage of mortar prisms was measured according to NM 10.1.005 [32]. The results (Table 11) indicate a slight reduction in shrinkage with increasing EAF-SS content. At 28 days, the reference OPC exhibited a shrinkage value of 630 μm/m, whereas BC2, BC3, BC5, BC10, and BC15 showed 625, 620, 610, 580, and 560 μm/m, respectively.

Table 11. Results of shrinkage tests.

Sample Code	Shrinkage (μm/m)			
	3 d	**7 d**	**14 d**	**28 d**
OPC	330 ± 5	430 ± 7	550 ± 9	630 ± 8
BC2	330 ± 5	428 ± 7	547 ± 9	625 ± 8
BC3	330 ± 6	420 ± 6	540 ± 7	620 ± 5
BC5	315 ± 6	410 ± 7	525 ± 6	610 ± 5
BC10	310 ± 7	400 ± 8	510 ± 8	580 ± 7
BC15	300 ± 5	390 ± 7	500 ± 6	560 ± 6

This reduction may be attributed to the physical characteristics of EAF-SS, particularly its relatively coarser particle size and lower hydraulic reactivity compared with clinker. Consistent with this interpretation, the water demand results reported in Section 3.4 (Table 8) show a progressive decrease in W/C ratio from 27.53% for OPC to 24.81% for BC15, indicating a reduced overall water requirement with increasing slag content. This lower water demand may limit internal moisture loss during hydration, thereby contributing to reduced shrinkage development.

Furthermore, the lower hydraulic reactivity of EAF-SS may reduce self-desiccation during the early curing period, potentially limiting internal stresses and shrinkage. It should be noted, however, that the reduction in drying shrinkage occurs alongside an increase in total open porosity in the blended systems. This behavior is not necessarily contradictory, since drying shrinkage depends not only on total pore volume but also on pore size distribution and capillary connectivity. A possible explanation is that the incorporation of EAF-SS modifies the pore network by reducing the fraction of fine capillary pores responsible for high capillary tension during drying, while increasing the proportion of coarser or less connected pores. Under such conditions, total porosity may increase whereas drying shrinkage decreases. However, as pore size distribution was not measured in the present study, this interpretation should be regarded as tentative.

Direct measurements of internal relative humidity, water retention, or pore size distribution were not performed in this study, and the proposed mechanisms should therefore be considered indicative rather than experimentally verified. Future work incorporating internal RH monitoring and pore-structure characterization (e.g., mercury intrusion porosimetry) would allow a more rigorous mechanistic interpretation.

Overall, incorporating Moroccan EAF-SS as a partial replacement of OPC slightly mitigated drying shrinkage over the first 28 days, while contributing to the broader objective of valorizing steel slag in cementitious systems. These results provide preliminary insight into the volume stability behavior of EAF-SS blended mortars. Additional durability investigations, including chloride penetration, sulfate resistance, and long-term microstructural analysis, are currently ongoing and will be reported in future work. Nevertheless, the present shrinkage results should be interpreted as evidence of reduced early-age drying shrinkage under the conditions investigated, rather than as a complete assessment of long-term dimensional stability, which requires dedicated soundness and expansion testing.

3.7. Sustainability Implications

Partial substitution of OPC with Moroccan EAF-SS offers a potential pathway to reduce CO_2 emissions from cement production while valorizing industrial by-products. The actual environmental benefits depend on factors such as energy requirements for slag processing, transportation distances, and any pretreatment applied. Therefore, the CO_2

savings discussed here should be considered preliminary indicators rather than a full life-cycle assessment (LCA).

Therefore, the sustainability assessment presented in this study should be considered a preliminary screening analysis intended to illustrate the potential environmental benefits of clinker substitution rather than a complete environmental evaluation.

3.7.1. Estimation of CO_2 Emission Savings

OPC was partially replaced with Moroccan EAF steel slag (EAF-SS) at 2%, 3%, 5%, 10%, and 15%. Because OPC production is clinker-intensive, this substitution can be interpreted as a reduction in clinker demand and associated process emissions.

As an industrial by-product, EAF-SS does not require calcination, and its direct CO_2 emissions are negligible compared with clinker. Importantly, the direct use of untreated EAF-SS without any mechanical or chemical activation eliminates pretreatment energy costs, representing an energetic advantage over activated slag systems and partially offsetting the energy associated with slag transportation and grinding.

Using the mass-based approach recommended by IPCC (2006) [48,49] EN 16757:2017, CO_2 savings were estimated as:

$$CO_2 \text{ savings} = \text{frep} \times \text{EFclinker}$$

where

CO_2 savings = reduction in CO_2 emissions (tCO_2 per ton of cement)
frep = clinker replacement fraction
EFclinker = emission factor for clinker production (tCO_2 per ton clinker)

Assuming EFclinker = 0.85 t CO_2/t clinker, the estimated savings per ton of cement are shown in Table 12. For mechanically compliant mixtures (2–5% EAF-SS, 42.5R), CO_2 savings are 17–26 kg/t cement. Based on the adopted assumptions, the theoretical CO_2 emission reduction associated with 15% clinker substitution may reach approximately 120–128 kg CO_2 per ton of cement.

Table 12. Estimated indicative CO_2 savings based on simplified mass-balance calculation.

Cement Type	OPC Replacement by EAF-SS (%)	Estimated CO_2 Savings (kg CO_2 per Ton Cement)
BC2	2	17
BC3	3	26
BC5	5	43
BC10	10	85
BC15	15	128

Note: these values represent approximate estimates based on a simplified mass-based calculation and do not include emissions associated with grinding energy, transportation, slag pretreatment, or additional processing. Consequently, the results should be interpreted as indicative rather than definitive environmental impacts, and a complete evaluation would require a full life-cycle assessment (LCA).

Sensitivity to clinker emission factor: Using 0.80–0.90 t CO_2/t clinker, estimated savings for 15% OPC replacement range from 120 to 135 kg/t cement, highlighting the dependence on plant-specific data.

Other considerations: Additional grinding energy for slag, transportation, or pretreatment may reduce net savings. If Moroccan steel industries produce ~196,000 t EAF-SS annually, valorization in cement could potentially reduce CO_2 emissions by 20,000–25,000 t

annually, depending on plant and processing conditions. These values are indicative; full life-cycle assessments (LCA) are needed for precise evaluation.

3.7.2. Contribution to the Circular Economy

Incorporating EAF steel slag into cement production contributes to the principles of the circular economy by transforming an industrial by-product into a valuable secondary raw material. The integration of EAF-SS reduces landfill disposal, mitigates environmental risks associated with slag accumulation, and promotes industrial symbiosis between the steel and construction sectors.

The potential diversion of slag from landfills can be quantified as follows:

$$\text{Slag Utilization Rate (\%)} = [\text{Mass of EAF-SS used in cement (t)}/\text{Total annual EAF-SS production (t)}] \times 100$$

Assuming a cement plant produces 1 million tons of cement annually with a 15% OPC replacement by EAF-SS, approximately 150,000 tons of EAF-SS could be consumed each year. Under the assumptions considered in this study, this would correspond to a potential valorization rate approaching 76% of the annual Moroccan EAF-SS production. This approach also supports the United Nations Sustainable Development Goals: SDG 9, which promotes industry, innovation, and infrastructure, and SDG 12, which encourages responsible consumption and production [50].

3.7.3. Overall Environmental Benefit

The combined effects of reduced OPC consumption, lower clinker demand, raw material conservation, and industrial waste valorization indicate that the use of Moroccan EAF steel slag as a partial OPC replacement appears to represent a promising strategy for improving the sustainability of cement production. While the simplified calculations presented in this study suggest potential environmental benefits, further research incorporating complete life-cycle assessment methodologies will be necessary to quantify the net environmental performance under real industrial conditions.

These findings are consistent with Morocco's national strategies for sustainable development and low-carbon transition, highlighting the potential role of EAF-SS in supporting more resource-efficient and circular cement production systems [51]. However, a full LCA incorporating grinding energy, transportation, and plant-specific emission factors will be necessary to precisely quantify the net environmental performance under real industrial conditions.

4. Comparative Assessment of EAF-SS with International Slags

To contextualize the characteristics of Moroccan EAF-SS, Table 13 compares its main chemical and physical properties with those reported for electric arc furnace steel slags from different regions in the literature. The international data were compiled from previously published studies on European and Chinese EAF steel slags used in cementitious systems [52–55].

The comparison highlights that Moroccan EAF-SS differs markedly from many EAF slags reported in the literature, particularly because of its exceptionally high Fe_2O_3 content and lower SiO_2 and MgO contents. These differences confirm that Moroccan EAF-SS should be considered a compositionally distinct slag rather than a representative average EAF slag. Nevertheless, its relatively high CaO and Fe_2O_3 contents remain broadly consistent with the general chemical characteristics of EAF slags produced during steel refining. Literature reports commonly describe EAF slags as containing calcium silicate phases together with ferrite- and RO-type phases; in the present study, XRD confirmed the presence of calcium

silicate phases and Fe-/Mg-bearing crystalline phases, although ferrite phases such as C_4AF were not clearly resolved.

Table 13. Comparative chemical and physical properties of Moroccan EAF-SS with international slags (data compiled from literature).

Chemical Composition (wt%)	SiO_2	Al_2O_3	Fe_2O_3	CaO	MgO	Free CaO	MnO	Density (g/cm^3)	SSA (m^2/g)	Main Phases
Moroccan EAF-SS	5.87	1.43	57.12	27.18	2.39	1–2	3.16	3.1–3.4	0.92	β-C_2S, C_3S, FeO, MgO, Fe-rich phases
European EAF-SS [53,54]	14–17	3–5	15–20	32–36	7–10	0.5–2	1–3	3.2–3.6	0.4–0.7	C_2S, RO phase, ferrite
Chinese EAF-SS [55,56]	13–16	4–7	16–20	34–40	6–9	1–3	2–4	3.2–3.5	0.5–0.9	C_2S, C_4AF, RO phase

These similarities indicate that Moroccan EAF-SS exhibits chemical and physical characteristics comparable to those of international EAF slags, which have previously been investigated as supplementary cementitious materials [52–55]. Furthermore, the use of EAF-SS as a partial OPC replacement has been reported to reduce CO_2 emissions, lower energy consumption, and promote circular economy strategies by valorizing industrial waste [56–59]. Consequently, the comparison not only supports the technical feasibility of incorporating Moroccan EAF-SS into blended cement systems but also highlights its potential environmental benefits, reinforcing the relevance of the mineralogical, physical, and sustainability analyses presented in this study.

5. Limitations and Future Works

This study demonstrates the technical feasibility and environmental benefits of incorporating untreated Moroccan electric arc furnace steel slag (EAF-SS) as a partial replacement of OPC in cement production. The mineralogical and chemical characteristics of EAF-SS were identified using XRD and X-ray fluorescence (XRF), and its influence on setting time, density, porosity, and mechanical properties was experimentally assessed.

Additional analytical limitations include the absence of Rietveld refinement for quantitative phase analysis, which would provide more accurate phase fractions and confirm C_2S polymorph distribution (β- vs. γ- vs. α'-C_2S). Amorphous phase content was not quantified, which limits the assessment of intrinsic slag reactivity. These analyses, including high-resolution XRD or Raman spectroscopy for polymorph identification and internal standard methods for amorphous quantification, are recommended in future work.

Direct pore solution analysis, including Ca^{2+} and Fe^{3+} ion concentration measurements, was not performed, limiting direct verification of the proposed Fe-rich phase dissolution mechanism. A formal statistical correlation between pore solution pH and setting time was not established, and the proposed mechanistic relationship remains a qualitative interpretation. Isothermal calorimetry and mercury intrusion porosimetry (MIP) are identified as priority measurements to directly assess hydration kinetics and pore size distribution.

A comparative experiment with an inert reference filler was not performed, which limits the decoupling of dilution effects from slag-specific chemical contributions to mechanical performance. Heavy metal leaching tests (Cr, Ni, Cu) following EN 12457-2: 2002 [60] protocols were not conducted, which represents a limitation for comprehensive environmental safety assessment and is explicitly planned as priority future work. Extended mechanical testing at 56, 90, and 180 days was not performed in this study; given that EAF slag is

known to contribute to late-age strength development, longer-term testing is identified as a key objective of ongoing work.

Furthermore, although the physico-mechanical behavior of the blended cements was thoroughly evaluated, no direct microstructural observations (e.g., scanning electron microscopy, SEM) were performed. As a result, interpretations of hydration evolution and the formation of microstructural products were partly inferred from established mechanisms reported in the literature. In addition, no thermogravimetric analysis (TGA) was conducted to quantify calcium hydroxide consumption and the development of hydration phases. Both SEM and TGA are planned in ongoing complementary work to strengthen the understanding of slag–cement interactions at the microstructural level.

Furthermore, the assessment of CO_2 emission reductions was based on a simplified mass-based calculation and does not constitute a complete life cycle assessment (LCA). A detailed LCA will be performed in future research to include energy consumption, slag processing, transportation, and plant-specific emission factors.

Finally, the long-term volumetric stability of untreated EAF-SS, including potential delayed expansion associated with free CaO and/or MgO hydration, was not directly evaluated in the present study by standard soundness tests such as autoclave expansion or Le Chatelier methods. This represents an important limitation, particularly for steel slag-based binders. Short-term dimensional behavior was assessed only through drying shrinkage measurements up to 28 days, which showed a slight reduction with increasing slag content (from 630 μm/m for OPC to 560 μm/m for BC15). However, these results should not be interpreted as a substitute for dedicated expansion or soundness testing, since drying shrinkage does not capture delayed expansive phenomena associated with periclase or free lime hydration. Ongoing durability investigations, including extended hydration and expansion measurements, are currently being conducted and will be reported in a subsequent publication.

Overall, future studies will focus on microstructural characterization (SEM, TGA), long-term durability assessment, and full LCA modeling to provide a more comprehensive evaluation of the performance, sustainability, and industrial applicability of Moroccan EAF-SS in cementitious systems.

6. Conclusions

This study evaluated the feasibility of incorporating untreated Moroccan electric arc furnace steel slag (EAF-SS) as a partial replacement of ordinary Portland cement (OPC) in blended cement systems. The slag exhibited an atypical chemical composition compared with many EAF slags reported in the literature, particularly its very high Fe_2O_3 content (~57 wt.%), highlighting the importance of source-specific characterization before valorization in cementitious materials.

The results showed that EAF-SS incorporation progressively modified binder composition by increasing Fe_2O_3, Al_2O_3, and MgO contents while slightly reducing CaO, without exceeding the EN 197-1 limits for SO_3 and loss on ignition in the investigated formulations. XRD analysis identified calcium silicate phases together with Fe- and Mg-bearing crystalline phases, providing a mineralogical framework for interpreting the observed behavior, although no quantitative phase refinement or amorphous-phase determination was performed.

From a performance perspective, increasing EAF-SS content reduced water demand but slightly delayed the initial setting time. Compressive strength decreased progressively with increasing replacement level, from 53 MPa for OPC to 36 MPa for BC15 at 28 days, while open porosity increased from 12% to 18%. A slight reduction in drying shrinkage was also observed as EAF-SS content increased. Under the investigated condi-

tions, blends containing 2–5 wt.% EAF-SS provided the most favorable balance between clinker-related material reduction and technical performance, while still satisfying the compressive-strength requirements associated with EN 197-1 class 42.5R. Higher replacement levels (10–15 wt.%) led to a marked reduction in mechanical performance and are therefore not recommended for 42.5R-equivalent applications based on the present results.

The combined physical, mineralogical, and mechanical results suggest that the coarser particle size, lower specific surface area, and phase assemblage of untreated EAF-SS contribute to lower early-age reactivity and reduced mechanical performance at higher replacement levels. However, these interpretations remain qualitative, since no direct microstructural or calorimetric analyses were performed to verify hydration mechanisms.

From a sustainability perspective, the use of untreated EAF-SS appears promising as a route for reducing OPC consumption and valorizing Moroccan steelmaking by-products within a circular economy framework. Nevertheless, the environmental assessment presented in this study remains preliminary and should be confirmed by full life-cycle assessment and leaching investigations.

Overall, the results indicate that untreated Moroccan EAF-SS can be incorporated at low replacement levels, particularly 2–5 wt.%, in blended cement systems without compromising the targeted strength class under the conditions investigated. Future work should focus on long-term performance, soundness and expansion behavior, durability, environmental safety, and direct microstructural characterization in order to clarify hydration mechanisms and confirm the long-term suitability of this slag for cementitious applications.

Author Contributions: Conceptualization, I.H. and A.N.; methodology, I.H. and A.N.; validation, I.H., A.N. and R.E.; formal analysis, I.H.; investigation, I.H.; resources, O.B.; data curation, O.B.; writing—original draft preparation, I.H.; writing—review and editing, A.N. and R.E.; visualization, I.H.; supervision, R.E.; project administration, I.H.; funding acquisition, this research received no external funding. All authors have read and agreed to the published version of the manuscript.

Funding: This research received no external funding.

Institutional Review Board Statement: Not applicable.

Informed Consent Statement: Not applicable.

Data Availability Statement: The data presented in this study are available from the corresponding author upon reasonable request.

Conflicts of Interest: The authors declare no conflicts of interest.

Abbreviations

The following abbreviations are used in this manuscript:

PC	Portland Cement
OPC	Ordinary Portland Cement
EAF	Electric Arc Furnace
EAF-SS	EAF-steel slags
SCM	Supplementary cementitious materials

References

1. Global Cement Staff. Global Cement Top 100 2026: World Cement Production Reached Approximately 4.00 billion Tonnes in 2024 According to USGS Estimates. Global Cement. 2025. Available online: https://www.globalcement.com/magazine/articles/1390-global-cement-top-100-2026 (accessed on 26 March 2026).
2. Global Cement News. Morocco: Cement Deliveries Reached 12.3 Million Tonnes at the End of October 2025. Global Cement. 2025. Available online: https://www.globalcement.com/news/20073-moroccan-cement-sales-up-by-11-in-october-2025 (accessed on 26 March 2026).

3. Sáez-de-Guinoa Vilaplana, A.; Ferreira, V.J.; López-Sabirón, A.M.; Aranda-Usón, A.; Lausín-González, C.; Berganza-Conde, C.; Ferreira, G. Utilization of ladle furnace slag from a steelwork for laboratory scale production of Portland cement. *Constr. Build. Mater.* **2015**, *94*, 837–843. [CrossRef]
4. Petroche, D.M.; Ramirez, A.D. The environmental profile of clinker, cement, and concrete: A life cycle perspective study based on Ecuadorian data. *Buildings* **2022**, *12*, 311. [CrossRef]
5. Sahoo, N.; Kumar, A.; Samsher. Review on energy conservation and emission reduction approaches for cement industry. *Environ. Dev.* **2022**, *44*, 100767. [CrossRef]
6. Martins, A.C.P.; Franco de Carvalho, J.M.; Costa, L.C.B.; Andrade, H.D.; de Melo, T.V.; Ribeiro, J.C.L.; Pedroti, L.G.; Peixoto, R.A.F. Steel slags in cement-based composites: An ultimate review on characterization, applications and performance. *Constr. Build. Mater.* **2021**, *291*, 123265. [CrossRef]
7. Moujoud, Z.; Sair, S.; Ait Ousaleh, H.; Ayouch, I.; El Bouari, A.; Tanane, O. Geopolymer composites reinforced with natural fibers: A review of recent advances in processing and properties. *Constr. Build. Mater.* **2023**, *388*, 131666. [CrossRef]
8. Andrew, R.M. Global CO_2 emissions from cement production. *Earth Syst. Sci. Data* **2018**, *10*, 195–217. [CrossRef]
9. Nandhini, K.; Karthikeyan, J. A review on sustainable production of self-compacting concrete utilizing industrial by-products as cementitious materials. *Innov. Infrastruct. Solut.* **2022**, *7*, 199.
10. Zeng, Q.; Liu, X.; Zhang, Z.; Wei, C.; Xu, C. Synergistic utilization of blast furnace slag with other industrial solid wastes in cement and concrete industry: Synergistic mechanisms, applications, and challenges. *Green Energy Resour.* **2023**, *1*, 100012. [CrossRef]
11. Li, X.; Qin, D.; Hu, Y.; Ahmad, W.; Ahmad, A.; Aslam, F.; Joyklad, P. A systematic review of waste materials in cement-based composites for construction applications. *J. Build. Eng.* **2022**, *45*, 103447. [CrossRef]
12. Onyenokporo, N.C. Supplementary cementitious materials as sustainable partial replacement for cement in the building industry. *Int. J. Archit. Environ. Eng.* **2022**, *16*, 74–84.
13. Subramaniam, D.N.; Sathiparan, N. Comparative study of fly ash and rice husk ash as cement replacement in pervious concrete: Mechanical characteristics and sustainability analysis. *Int. J. Pavement Eng.* **2022**, *24*, 2075867. [CrossRef]
14. Teixeira, E.R.; Camões, A.; Branco, F.G.; Aguiar, J.B.; Fangueiro, R. Recycling of biomass and coal fly ash as cement replacement material and its effect on hydration and carbonation of concrete. *Waste Manag.* **2019**, *94*, 39–48. [CrossRef] [PubMed]
15. Yoon, H.N.; Seo, J.; Kim, S.; Lee, H.K.; Park, S. Characterization of blast furnace slag-blended Portland cement for immobilization of Co. *Cem. Concr. Res.* **2020**, *134*, 106089. [CrossRef]
16. Xu, Y.; Liu, X.; Zhang, Y.; Tang, B.; Mukiza, E. Investigation on sulfate activation of electrolytic manganese residue on early activity of blast furnace slag in cement-based cementitious material. *Constr. Build. Mater.* **2019**, *229*, 116831. [CrossRef]
17. Zhang, Y.; Chang, J.; Zhao, Q.; Lam, W.L.; Shen, P.; Sun, Y.; Zhao, D.; Poon, C.S. Effect of dosage of silica fume on the macro-performance and micro/nanostructure of seawater Portland cement pastes prepared with an ultra-low water-to-binder ratio. *Cem. Concr. Compos.* **2022**, *133*, 104700.
18. Wang, Q.; Liu, R.; Liu, P.; Liu, C.; Sun, L.; Zhang, H. Effects of silica fume on the abrasion resistance of low-heat Portland cement concrete. *Constr. Build. Mater.* **2022**, *329*, 127165. [CrossRef]
19. World Steel Association. May 2023 Crude Steel Production. Available online: https://worldsteel.org/media-centre/press-releases/2023/may-2023-crude-steel-production/ (accessed on 26 June 2023).
20. Carvalho, V.R.; Costa, L.C.B.; Elói, F.P.D.F.; Bezerra, A.C.S.; de Carvalho, J.M.F.; Peixoto, R.A.F. Performance of low-energy steel slag powders as supplementary cementitious materials. *Constr. Build. Mater.* **2023**, *392*, 131888. [CrossRef]
21. Roslan, N.H.; Ismail, M.; Khalid, N.H.A.; Muhammad, B. Properties of concrete containing electric arc furnace steel slag and steel sludge. *J. Build. Eng.* **2020**, *28*, 101060. [CrossRef]
22. Wang, H.; Ouyang, S.; Lv, Y.; Chen, S.; Zhai, Z.; Wang, D.; Jin, W. Mechanical properties and microstructural mechanism of ternary geopolymer cementitious materials based on molybdenum tailings, red mud and GGBS. *Constr. Build. Mater.* **2026**, *510*, 145938. [CrossRef]
23. Lv, Y.; Liu, Z.; Ouyang, S.; Yuan, C.; Zhu, X.; Wang, M.; Li, H.; Jin, W. Preparation and performance of an all-solid-waste alkali-activated cementitious material incorporating molybdenum tailings, Bayer red mud, and calcium carbide slag. *Transp. Geotech.* **2026**, *60*, 102107. [CrossRef]
24. Jin, W.; Zhang, Y.; Sun, J.; Li, X.; Song, Z. Properties and microscopic mechanism of MKP-modified magnesium oxychloride cement solidified red mud. *Dev. Built Environ.* **2025**, *24*, 100774. [CrossRef]
25. Gao, T.; Dai, T.; Shen, L.; Jiang, L. Benefits of using steel slag in cement clinker production for environmental conservation and economic revenue generation. *J. Clean. Prod.* **2021**, *282*, 124538. [CrossRef]
26. Bullerjahn, F.; Bolte, G. Composition of the reactivity of engineered slags from bauxite residue and steel slag smelting and use as SCM for Portland cement. *Constr. Build. Mater.* **2022**, *321*, 126331. [CrossRef]
27. Martins, A.C.P.; de Carvalho, J.M.F.; Duarte, M.D.N.; de Lima, G.E.S.; Pedroti, L.G.; Peixoto, R.A.F. Influence of a LAS-based modifying admixture on cement-based composites containing steel slag powder. *J. Build. Eng.* **2022**, *53*, 104517. [CrossRef]

28. Wang, Y.; Suraneni, P. Experimental methods to determine the feasibility of steel slags as supplementary cementitious materials. *Constr. Build. Mater.* **2019**, *204*, 458–467. [CrossRef]
29. Rui, Y.; Qian, C. CO_2-fixing steel slag on hydration characteristics of cement-based materials. *Constr. Build. Mater.* **2022**, *354*, 129193. [CrossRef]
30. Rui, Y.; Qian, C.; Zhang, X.; Ma, Z. Different carbon treatments for steel slag powder and their subsequent effects on properties of cement-based materials. *J. Clean. Prod.* **2022**, *362*, 132407. [CrossRef]
31. *NF P 18-459*; Concrete—Determination of Water-Accessible Porosity and Apparent Density of Hardened Concrete. AFNOR: Paris, France, 2010.
32. *NM 10.1.005*; Hydraulic Binders—Testing Methods. Moroccan Institute for Standardization (IMANOR): Rabat, Morocco, 2008.
33. Nguyen, K.-S.; Phuoc, N.V.; Hanh, L.T.D.; Minh, H.N.; Son, L.M.; Hoa, N.T. EAF Steel Slag as Supplementary Cementing Material. *ASEAN Eng. J.* **2015**, *4*, 34–43. [CrossRef]
34. Andersson, A.; Isaksson, J.; Lennartsson, A.; Engström, F. Insights into the Valorization of Electric Arc Furnace Slags as Supplementary Cementitious Materials. *J. Sustain. Metall.* **2023**, *10*, 96–109. [CrossRef]
35. Liu, X.; Wu, P.; Liu, X.; Zhang, Z.; Ai, X. The Utilization of Carbonated Steel Slag as a Supplementary Cementitious Material in Cement. *Materials* **2024**, *17*, 4574. [CrossRef] [PubMed]
36. Hooton, R.D.; Emery, J.J. Sulfur distribution in granulated iron blast furnace slags. *Can. Metall. Q.* **1983**, *22*, 291–297.
37. *EN 197-1:2011*; Cement–Part 1: Composition, Specifications and Conformity Criteria for Common Cements. European Committee for Standardization (CEN): Brussels, Belgium, 2011.
38. Cullity, B.D.; Stock, S.R. *Elements of X-Ray Diffraction*, 3rd ed.; Prentice Hall: Upper Saddle River, NJ, USA, 2001.
39. Mohammed, S.; Safiullah, O. Optimization of the SO_3 content of an Algerian Portland cement: Study on the effect of various amounts of gypsum on cement properties. *Constr. Build. Mater.* **2018**, *164*, 362–370. [CrossRef]
40. Zhuang, S.; Wang, Q.; Luo, T. Effect of C12A7 in steel slag on the early-age hydration of cement. *Cem. Concr. Res.* **2022**, *162*, 107010. [CrossRef]
41. Zhuang, S.; Wang, Q. Inhibition mechanisms of steel slag on the early-age hydration of cement. *Cem. Concr. Res.* **2021**, *140*, 106283. [CrossRef]
42. Suraneni, P.; Palacios, M.; Flatt, R.J. New insights into the hydration of slag in alkaline media using a micro-reactor approach. *Cem. Concr. Res.* **2016**, *79*, 209–216. [CrossRef]
43. Chen, Z.; Ye, H. The role of CaO and MgO incorporation in chloride resistance of sodium carbonate-activated slag. *Cem. Concr. Compos.* **2022**, *132*, 104625.
44. Shi, C.; Qian, J. High performance cementing materials from industrial slags—A review. *Resour. Conserv. Recycl.* **2000**, *29*, 195–207. [CrossRef]
45. Han, F.; Zhang, Z.; Wang, D.; Yan, P. Hydration heat evolution and kinetics of blended cement containing steel slag at different temperatures. *Thermochim. Acta* **2015**, *605*, 43–51. [CrossRef]
46. Qasrawi, H.; Asi, I. Effect of EAF Steel Slag Aggregate on Concrete Properties. *Constr. Build. Mater.* **2010**, *24*, 984–990.
47. Pellegrino, C.; Faleschini, F. Experimental Behavior of Concrete with EAF Steel Slag as Cement Replacement. *Constr. Build. Mater.* **2016**, *121*, 354–364.
48. IPCC. *2006 IPCC Guidelines for National Greenhouse Gas Inventories*; Institute for Global Environmental Strategies (IGES): Hayama, Japan, 2006.
49. *EN 16757:2017*; Sustainability of Construction Works—Environmental Product Declarations—Product Category Rules for Concrete and Concrete Elements. European Committee for Standardization (CEN): Brussels, Belgium, 2017.
50. United Nations. *Transforming Our World: The 2030 Agenda for Sustainable Development*; United Nations: New York, NY, USA, 2015.
51. Kingdom of Morocco. *National Strategy for Sustainable Development (Stratégie Nationale de Développement Durable—SNDD)*; Ministry of Energy, Mines and Sustainable Development: Rabat, Morocco, 2017.
52. Motz, H.; Geiseler, J. Products of Steel Slags: Their Development and Use. *Waste Manag.* **2001**, *21*, 285–293. [PubMed]
53. Shi, C. Characteristics and cementitious properties of ladle slag fines from steel production. *Cem. Concr. Res.* **2002**, *32*, 459–462. [CrossRef]
54. Guo, X.; Shi, H.; Dick, W.A. Compressive strength and microstructural characteristics of class C fly ash geopolymer. *Constr. Build. Mater.* **2010**, *24*, 1126–1132. [CrossRef]
55. Wang, Q.; Yan, P.; Yang, J. Hydration properties of basic oxygen furnace steel slag. *Constr. Build. Mater.* **2011**, *25*, 132–138. [CrossRef]
56. Habert, G.; d'Espinose de Lacaillerie, J.B.; Roussel, N. An environmental evaluation of geopolymer based concrete production: Reviewing current research trends. *J. Clean. Prod.* **2011**, *19*, 1229–1238. [CrossRef]
57. Zhang, P.; Jiang, T.; Xu, S.; Wang, S.; Wang, Y. Environmental benefits of steel slag utilization in cement and concrete: A review. *Resour. Conserv. Recycl.* **2020**, *155*, 104632. [CrossRef]

58. Li, C.; Zhao, Z.; Wang, K.; Chen, H. Life cycle assessment of cementitious composites incorporating industrial by-products: Energy and CO_2 reductions. *J. Clean. Prod.* **2019**, *220*, 1051–1062. [CrossRef]
59. Siddique, R.; Klaus, J. Influence of slag as partial replacement of cement on the environmental footprint of concrete. *Waste Manag.* **2009**, *29*, 2973–2978. [CrossRef] [PubMed]
60. *EN 12457-2:2002*; Characterization of Waste—Leaching—Compliance Test for Leaching of Granular Waste Materials and Sludges—Part 2: One Stage Batch Test at a Liquid-to-Solid Ratio of 10 L/kg for Materials with Particle Size Below 4 mm (Without or with Size Reduction). European Committee for Standardization (CEN): Brussels, Belgium, 2002.

Disclaimer/Publisher's Note: The statements, opinions and data contained in all publications are solely those of the individual author(s) and contributor(s) and not of MDPI and/or the editor(s). MDPI and/or the editor(s) disclaim responsibility for any injury to people or property resulting from any ideas, methods, instructions or products referred to in the content.